NATIONAL ADVISORY COMMITTEE FOR AERONAUTICS

TECHNICAL NOTE 2827

INVESTIGATION OF A DIFFRACTION-GRATING INTERFEROMETER FOR USE IN AERODYNAMIC RESEARCH

By James R. Sterrett and John R. Erwin

Langley Aeronautical Laboratory
Langley Field, Va.

Washington
November 1952

NATIONAL ADVISORY COMMITTEE FOR AERONAUTICS

TECHNICAL NOTE 2827

INVESTIGATION OF A DIFFRACTION-GRATING INTERFEROMETER FOR USE IN AERODYNAMIC RESEARCH

By James R. Sterrett and John R. Erwin

SUMMARY

A low-cost interferometer that is easy to adjust and has a large field of view is described. This instrument, which is based on a principle discovered by Kraushaar, uses small diffraction gratings to produce and recombine separate beams of light. The usual two-parabolic-mirror schlieren system can be converted inexpensively to a diffraction-grating interferometer.

Experimental data are presented to verify the ability of the instrument to provide valid and reliable measurements of air density. Photographs of the flow in a supersonic cascade tunnel are included to indicate the quality of the interferograms obtained.

INTRODUCTION

The Mach-Zehnder interferometer has been used in many phases of aerodynamic research. The cost of this instrument is high because of the size, number, and accuracy required of the optical components and alining mechanisms. The adjustment of the components is exacting because the four flat optical elements must be positioned with great precision. The diffraction-grating interferometer discovered by Kraushaar (ref. 1) is not subject to these limitations. Although similar in construction to the apparatus used in the grid-screen (Ronchi) method (ref. 2), the grating interferometer works on entirely different physical principles. In this instrument, light is separated into discrete beams and recombined by small diffraction gratings to produce optical interference. The adjustment of the optical elements is easy because the two light beams are reflected or diffracted by the same elements. The usual two-parabolic-mirror schlieren system can be converted inexpensively into a diffraction-grating interferometer. The potential size of the view field is apparently limited only by the size of the parabolic mirrors.

This paper presents the physical principles of the diffraction-grating interferometer and describes an instrument which employs simple,

easily procured equipment. A technique of adjustment is given. Several experiments conducted to determine both the validity and the reliability of the data obtained are described. An existing schlieren system used with a supersonic cascade tunnel was also converted to an interferometer. Photographs of the flow around a model in this tunnel are included to illustrate the quality of the interferograms obtained. Inasmuch as the references listed give ample information concerning the interference method, only that part of the theory necessary for clarity in describing the diffraction-grating interferometer is presented.

SYMBOLS

b	undisturbed fringe spacing
d	grating constant - width of transparent and opaque intervals of grating
f	focal length of lens
i	angle of incidence
k	Gladstone-Dale constant
L	distance light travels through disturbance
n	order of diffraction beam
S	fringe shift in terms of undisplaced fringe width
T	temperature of air outside thermal boundary layer
T'	temperature of plate and of air immediately at surface of plate
x	distance from grating to focal point of lens
α	angle between recombining light beams
β, β_1, β_2	angles subtended by light rays in diffraction-grating interferometer
θ	angle of diffraction
λ	wavelength of light
λ_o	wavelength of light in vacuum
μ	index of refraction of air of density ρ

ρ density of air in undisturbed field

ρ' density of air at any position in disturbed field

ω diffraction angle of ray perpendicular to grating

Subscripts:

i data calculated from interferometer measurements

n order of diffraction beam

s data calculated from temperature and pressure measurements

THEORY AND USE OF THE DIFFRACTION-GRATING INTERFEROMETER

Theory

Mach-Zehnder interferometer.- Figure 1 shows a schematic drawing of the usual Mach-Zehnder interferometer. A variation of this type of interferometer is described in reference 3. Unless otherwise noted, strictly monochromatic light from an infinitesimal source is assumed. Light from a single source passes around the two equal-length paths of the interferometer and is recombined to produce interference fringes. If the recombining beams are not inclined to each other, the rays will interfere and form the so-called infinite fringe (a single fringe). If the two recombining beams cross each other at a very small angle, finite fringes will be formed as shown in figure 2, in which two beams of parallel light are assumed to recombine. The wave fronts are represented as equally spaced straight lines in this figure. The number of fringes is determined by the angle between the two beams for any particular wavelength of light.

Diffraction-grating interferometer.- The theory of diffraction gratings has been given in many books (for example, refs. 4 and 5). Some of the important characteristics that are useful in understanding the grating interferometer are repeated herein for convenience. When a light beam is passed through a diffraction grating, as illustrated in figure 3, a series of diffracted beams are formed which obey the grating equation

$$\theta_n = \sin^{-1}\left(\frac{n\lambda}{d} + \sin i\right) \tag{1}$$

The sign convention is such that i is always considered positive; θ is considered positive when a ray crosses a line normal to the grating at the intersection of the ray and the grating (see fig. 3). In this equation, n is the order of the light beam and has positive and negative integral values, λ is the wavelength, d is the grating constant, i is the angle of incidence, and θ_n is the angle of diffraction. The grating constant d is generally given as the reciprocal of the number of lines per inch. The width of the wave front in each of the orders drawn in figure 3 varies. If the light beam passing through the grating is a divergent beam, the angle of incidence varies for the individual rays that make up the beam. In general, the deviation angles $\theta_n - i$ for the individual rays in any order vary slightly, except in the zero order.

The diffraction-grating interferometer uses a grating to produce two light beams which are later recombined by another grating to produce interference fringes. In figure 4, which for clarity has been drawn as a lens system, divergent light from a source is collected by a condenser lens L_1. This lens focuses the light on the diffraction grating G_1 after part of the light is cut off by the stop T. Angle β_1 is approximately equal to angle ω where angle ω equals $\theta_{n=-1}$ for the ray perpendicular to the grating. The 0 order is collimated by the bottom part of the lens L_2; similarly, the -1 order is collimated by the top part of the lens L_2. These two beams are collected by lens L_3, which is similar to lens L_2, and are refocused on the second grating G_2, which is placed near the image of the first grating. Thus, angle β_2 equals angle β_1. Since lenses L_2 and L_3 have the same focal length, the grating G_2 is chosen to have the same grating constant as G_1. The lines of G_2 are placed parallel to those of G_1. Many images resulting from both the 0 and -1 orders are formed at the plate (at B - B) by diffraction at G_2 (only four are drawn in fig. 4).

The following examples illustrate the convention that is used to refer to the different orders after the second grating. The 0 order of the beam of -1 order is designated as $(-1)_0$; similarly, the two first orders are designated as $(-1)_1$ and $(-1)_{-1}$. Each image from the original 0 beam overlaps with another image of the original -1 beam. For example, as shown in the insert in figure 4, the $(0)_{-1}$ order combines with the $(-1)_0$ order. Since the path lengths of the two recombining beams are approximately equal, interference will occur in each image where the different orders overlap. Since only one image is desired, consider only the image where the $(0)_{-1}$ beam combines with the $(-1)_0$ beam. Angle β_2 equals angle β_1 and the grating constant of G_2 is the same as that of G_1. When the second grating G_2 is placed at the image of G_1, the geometry of the system is such that the two recombining beams are not inclined to one another and the infinite fringe pattern results.

Figure 5(a) shows an enlarged cross section of the rays at the second grating for an infinite fringe. If the second grating is moved away from the image of the first grating, the rays of the $(-1)_0$ order remain unchanged (fig. 5(b)). The direction of the rays in the $(0)_{-1}$ beam remains unchanged, but the distance of any particular ray from the principal optical axis of the system has changed at the film plate. Thus, at the film plate, two different rays of the two orders recombine at a small angle and the two recombining beams appear to have different sources as is shown in figure 5(b). The number of fringes can thus be changed by moving the second grating in relation to the image of the first grating. The actual distances in figure 5(b) have been greatly exaggerated.

Use of white light.- In the appendix the fringe spacing for a grating interferometer is shown, analytically and experimentally, to be independent of the wavelength of light to a first approximation. Thus, when white light was used with the grating interferometer, a large number of multicolored fringes, with the colors located in the same relative position at each fringe, were obtained over the complete undisturbed view field. The fringes for the different colors were not superimposed. For example, when the interferometer was adjusted for a few fringes, the pattern on the screen was similar to a color spectrum at each fringe. The fringes were noticeable mainly because of the difference in color instead of a contrast between light and dark. The formation of a large number of white-light fringes with a grating interferometer is different from a Mach-Zehnder interferometer where the fringe spacing is a function of the wavelength of light.

In general, white light is not used for quantitative studies because the fringe shift is a function of the wavelength of light. This fact will be self-evident upon inspection of equation (2) which is stated subsequently in a discussion of the evaluation of interferograms. However, a broad-wavelength light source, which is desirable for the resulting high intensity, can be used for quantitative work.

Use of a finite light source.- In the previous discussion, light from an infinitesimal source was assumed. In practice, neither strictly monochromatic light nor light from a true point can be used because of the resulting low intensity. In the theory of a Mach-Zehnder interferometer, Schardin (ref. 6) has shown and many other investigators (for example, refs. 7 and 8) have noted the following experience to be true. If an ideal monochromatic mathematical point source could be used, fringes could be easily obtained with a very rough adjustment of the optical parts. In the practical case where an extended light source is used, the adjustment is more difficult because the same sections of the wave fronts should be recombined. In general, one plate and one mirror of the Mach-Zehnder interferometer are so adjusted that the two beams

appear to cross at the disturbance, and thus the same sections of the wave front recombine (note fig. 1).

Since a finite light source is used with the grating interferometer, a similar problem exists. Care must be taken to give the two recombining wave fronts the same optical treatment. It was noted experimentally that the quality of the fringes varied in the different images of the diffraction-grating interferometer. The most distinct fringes appear in the image which corresponds in figure 4 to the image formed when the $(-1)_0$ order combines with the $(0)_{-1}$ order. Each of these particular beams has passed through a grating as a zero order and as a first order of the same sign. The beams have received what might be termed conjugate optical treatment, and similar wave fronts exist after the second grating. When the lines of the second grating are placed parallel to the lines of the first grating, the same sections of the two wave fronts recombine when the second grating is placed at the image of the first grating. If the lines of the second grating are rotated or the grating is moved relative to the image of the first grating, the same sections of the wave fronts are moved relative to each other. The effect of such a misalinement is determined partially by the size of the light source. In general, the adjustment of the system is made easier when the size of the light source is reduced. This reduction in size, of course, reduces the amount of light that is available.

Construction of Interferometers

Two interferometers were actually built. Except for the focal length of the mirrors, the two were very similar. The interferometer which was used for development work is shown schematically in figure 6. A photograph of the apparatus is presented as figure 7. The instrument, as stated before, was constructed from available schlieren optics. Twelve-inch-diameter parabolic mirrors with a focal length of 96 inches were used (the focal length of the mirrors used with the other interferometer was 48 inches). The mirrors were mounted on a steel beam. Each grating was mounted so as to permit rotation about and translation along three mutually perpendicular axes (one axis is parallel to the optical axis of the system); an astrocompass and a microscope holder were used to make these adjustments. The fineness of the translational adjustments required is of the order of ± 0.01 inch, and the fineness of the rotation required is of the order of $\pm 0.25^\circ$. Two small plane front-surface mirrors were mounted on rods fastened to the steel beam. The steel beam was supported by three stands resting on foam-rubber pads. The light source and monochromator were mounted on a separate stand which was supported on foam-rubber pads. When large machinery was operated in the building, vibrations which traveled through the floor of the building caused the

fringe field to vibrate at a low frequency on the view screen. This vibration has not been a serious handicap because in all the photographs the short-duration light stopped all motion.

Commercial replica transmission gratings approximately 3/4 inch square with 2,000 lines per inch were used. Reflection gratings would have been convenient because the plane mirrors could have been eliminated. In general, the intensity of the first five orders on each side of the zero order was relatively high. The intensity of the first orders was slightly higher than that of the zero order when green light was used. The intensities of the first orders and the zero order were approximately equal for red light. When blue light was passed through the grating, the intensity of the first orders was many times the intensity of the zero order. (For a further description of this type of grating, see the section about the laminary grating, p. 248 of ref. 4). The zero and first orders for any particular ray were separated by approximately 4 inches at the parabolic mirrors. The light was stopped down near the condenser lens L_1 to keep the rays of the different orders from overlapping. The view field that resulted was approximately 4 inches by 11 inches. The grating constant for maximum utilization of the parabolic mirrors can be determined from equation (1). All orders after the first grating, except the zero and one of the first orders, were removed by covering part of the first parabolic mirror as shown in figure 6. If the other orders were not removed, undesired light from the other orders would appear in the usable field on the photograph.

The light source used was a General Electric B-H6 mercury lamp. The lamp can either be flashed or operated continuously. In most instances, the interferograms presented in this paper were obtained by discharging a 2.5-microfarad condenser charged to approximately 2,000 volts through the lamp. The effective time duration of the flash is believed to be less than 5 microseconds.

A prism-type Perkin-Elmer Corp. Universal Monochromator (model 83) was used. It was noted visually that fringes of comparable contrast and intensity could be obtained by using conventional light filters. The monochromator was adjusted to pass the green line in the mercury spectrum which has a wavelength of 5,460 angstroms. The width of the monochromator slits was set at 0.07 inch which passed the complete width of the light source. This setting, of course, allowed a certain amount of the continuous spectrum to pass through the monochromator. The exit slit of the monochromator is approximately 3/8 inch long, and this total length was used with the 96-inch focal-length mirrors. This length was reduced to 1/4 inch when the 48-inch focal-length mirrors were used.

The film used was Kodak Super XX. The film was slightly overdeveloped to yield normal negative density. The size of the image on the film was approximately one quarter of the original size.

The effective light source and the image of the light source were placed near the principal optical axis to minimize any astigmatic effects. A small shadow of the front-surface mirrors and grating mounts therefore occurred in the view field. It was noted experimentally that fringes could be obtained with an off-axis system.

The surface accuracy of the parabolic mirrors is greater than ±1/6 wavelength of light. Accuracy is easier and cheaper to obtain on a parabolic mirror than on a flat surface such as a splitter plate. The lenses used after the monochromator are simple lenses. The accuracy of the front-surface plane mirrors is not critical because of their position in the system. The first mirror is used before the beams are split and the second mirror occurs after the beams are recombined.

Adjustment of Interferometer

The interferometer is relatively easy to assemble and adjust; in fact, the complete optics of the system shown in figure 7 can be dismantled, reassembled, and adjusted within several hours by an experienced operator. The interferometer with the 96-inch focal-length mirrors was easier to adjust than the 48-inch focal-length mirror system. In the initial adjustment, the apparatus was first set up as if it were a schlieren system without a knife edge (the two gratings and all light stops were left out). The light from the monochromator exit slit was focused near the principal optical axis in front of the first plane mirror (see fig. 6). The usual schlieren adjustments were made to obtain an on-axis system with a parallel beam through the test section. The light-source image after the second parabolic mirror was refocused on the principal optical axis. If the effective light source is placed on the optical axis and the source image after the second parabolic mirror is sufficiently offset, curved fringes will result. The first grating was then placed approximately at the image of the slit. The desired dividing lines between the resulting orders will be parallel to the lines of the grating. The light was then stopped down in the vicinity of lens L_1 until the different orders did not overlap, and the dividing line between the zero and one of the first orders was on the center line of the mirror. Parts of the first parabolic mirror were covered to remove all orders except the two desired orders.

The second grating was then placed near the image of the first grating. This can be easily accomplished since the first grating was placed at the image of the light source. All adjustments up to now have been approximate and made only by eye. Fringes are now obtained by watching the screen and rotating the lines of the second grating slightly and moving the second grating slightly in relation to the image of the first grating. This trial-and-error method is made much easier by

masking the effective light source down to a very small source (as small as the intensity will allow). With this trial-and-error method, an experienced operator can usually obtain fringes in less than 15 minutes.

Once fringes are obtained, the masking of the effective light source is removed, and the lines of the second grating are rotated until well-defined fringes are obtained. The second grating is rotated slightly in each of three mutually perpendicular directions until fringes of maximum contrast are obtained. None of these adjustments are precision adjustments such as are characteristic of the adjustments made with a Mach-Zehnder interferometer. This ease of adjustment is explained by the fact that the two light beams are always reflected or diffracted from the same physical elements.

An adjustment technique which is not always needed is given as follows. The second grating is moved until a complete change of fringe spacing is observed on both sides of the image of the first grating. If the fringes appear to be more distinct when the second grating is located on one side of the image of the first grating than when on the other, it is a good indication that the angles which correspond to angles β_1 and β_2 in figure 4 are not equal (the light between the two parabolic mirrors is not parallel). To correct this condition, the distance from the first grating to the first parabolic mirror is changed slowly until fringes of similar quality are obtained when the second grating is located on either side of the image of the first grating.

The image used is the one which corresponds in figure 4 to the image formed when the $(-1)_0$ order combines with the $(0)_{-1}$ order because the most distinct fringes are formed in this image. The disturbance is located in the (-1) order so that its image will be aberration-free when it appears in the $(-1)_0$ order. The importance of the location of the disturbances follows from equation (1) and figure 3 which show that only the zero order is aberration-free. The disturbance area is focused on the viewing screen as in the usual schlieren system.

The fringes appear parallel to the lines of the grating (when a line source is used). Several examples of undisturbed fringes are shown in figures 8 and 9. Three of the images that result at the film plate are shown in figure 8. The images overlap slightly. The desired number of fringes is obtained by moving the second grating relative to the image of the first grating along the optical axis. Figure 9 shows typical examples of interferograms obtained with different fringe spacings. The contrast of the fringes decreases as the number of fringes is increased.

Evaluation of Interferograms

The theory of the evaluation of interferograms taken with a Mach-Zehnder interferometer is given in references 6 to 12. The general equation for two-dimensional analysis may be written as

$$\frac{\rho'}{\rho} = S \frac{\lambda_o}{L(\mu - 1)} + 1 \tag{2}$$

where for air it can be assumed that

$$\mu - 1 = k\rho \tag{3}$$

In these equations, ρ' is the density at any position in the disturbance field, ρ is the density in the undisturbed field, λ_o is the wavelength of light in a vacuum, L is the distance light travels through the disturbance, μ is the index of refraction of air of density ρ, k is the Gladstone-Dale constant for the wavelength λ_o, and S is the fringe shift in terms of undisplaced fringe width. The value of k was taken as 0.11663 cubic foot per slug for 5,460 angstroms.

The value S is determined from the interferograms. The density or fringe shift at some arbitrary reference point in the field must be known. When the interferometer is adjusted for the infinite fringe, S at any point is obtained by finding the number of interference fringes between the desired point and the reference point. This number is added or subtracted from the reference-point fringe shift, depending upon the direction of density change. For the infinite-fringe adjustment, the fringes are contours of equal density for two-dimensional disturbances. If the interferometer is set for finite fringes, the fringe shift may be obtained by comparing the interferograms taken with and without disturbances. A graphical technique for determining the fringe shift is given in reference 7. A photographic technique for determining lines of equal fringe shift by superimposing the negatives of the disturbed and undisturbed photographs is given in references 9 and 10. One of these three methods, whichever appeared most applicable for the particular problem, has been used to evaluate the interferograms given in this report.

The interferometer measures only the density of a gas. Often the other variables of the gas, such as temperature, velocity, and pressure, must be known. In general, one or more variables besides the density must be known or measured, and then from the fundamental gas laws, the other variables may be calculated. In wind-tunnel applications, these additional variables are often the stagnation temperature and pressure which are measured in the settling chamber. Shock losses can be estimated to good approximation by existing shock equations.

EXPERIMENTAL VERIFICATION

Temperature of a Heated Plate

Several tests were conducted to determine experimentally whether a grating interferometer measures the density directly, as does a Mach-Zehnder interferometer. The investigation of the large boundary layer on a heated plate is a convenient method to check the validity of the data obtained with the grating interferometer in a field with a density gradient. The temperature field around a heated plate has been determined experimentally by several investigators. Eckert and Soehngen in reference 11 investigated the laminar thermal convection boundary layer on a heated plate by the use of a Mach-Zehnder interferometer. It has been shown that the temperature of the air immediately at the surface of the plate is the same as the plate temperature. The temperature falls rapidly as the distance from the plate is increased. If the temperature of the air is plotted against the perpendicular distance from the plate, the temperature profile adjacent to the plate will approximate a straight line. By linear extrapolation the fringe number at the plate surface can be obtained.

A $\frac{5}{32}$-inch-thick copper plate with a height of 11 inches and a length L of 13.03 inches was placed to form one vertical side of a rectangular box containing an infrared bulb. The plate temperature was varied by changing the temperature of the box. The heat conduction of the copper maintained a constant temperature over the entire surface of the plate. This was verified experimentally by thermocouple measurements. The plate was placed with the length L in the direction of the light rays. Convection currents in the room were reduced to a minimum in order to maintain a laminar boundary layer. The interferometer was adjusted for the infinite fringe. Exact adjustment of the interferometer for the infinite fringe was difficult because of convection currents in the room, imperfections of the optical parts, and small vibrations of the system. However, the accuracy of the infinite-fringe method as used herein is believed to be within $\pm 1/4$ fringe shift.

Several interferograms of the field around the plate at different temperatures are shown in figure 10; T' is the temperature of the plate and T is the temperature of the air outside the boundary layer and, in this case, is the temperature of the air in the reference beam. The shadow near the top of the plate is caused by a device used to aline the plate with the light rays. The rectangular shadows on the left side of the photographs are the glass mountings for the gratings. Since the interferometer is adjusted for the infinite fringe, any fringe line is a constant-density line for two-dimensional disturbances. The pressure in the complete view field is approximately constant because of the low convection

velocities; thus the fringe lines may be considered as isotherms in the two-dimensional case since $\frac{T}{T'} = \frac{\rho'}{\rho}$.

The ends of the copper plate also heat the surrounding air, and the interferograms are therefore not strictly two-dimensional disturbances. For calculation purposes, an end-effect correction for the length L was obtained. From the interferograms, the fringe number was plotted against the perpendicular distance from the plate. The area under this curve was divided by the fringe number at the wall. Twice the resulting distance was added to the measured length of the plate. This correction gave an average distance L which would exist if the density along the light rays was the same at all points as it was at the surface of the plate. This correction further assumes that the boundary layer on the end of the plate along the light rays, which just touch the front surface of the plate, is the same as the boundary layer on the plate. As an example of the magnitude of this correction, the correction factor applied to the ratio ρ'/ρ when the temperature difference between room and plate was 46° F was less than 0.2 percent. Since the magnitude of the correction factor for end effects is small, the method used to correct for three-dimensional effects is sufficiently accurate.

Figure 11 shows the difference between the density of the air at the surface of the plate as calculated from interferometer measurements and the density at the plate as calculated from plate-temperature measurements. These differences are shown for two distances from the lower edge of the plate. Except for two points taken with a very low temperature difference, the average difference between densities determined by the two methods is approximately 0.3 percent. These differences are believed to be within the limitations of the accuracy of the checking method. The results of this test indicate that the data obtained with a grating interferometer are valid density measurements.

Measurements of Density Within a Box

Another method used to check the validity of the data obtained with a grating interferometer was to measure the known density of air in a box with glass sides. The box was divided into two compartments. The reference light beam passed through one compartment which was open to room conditions. The other light beam passed through the other compartment. The pressure in this compartment was varied and the density calculated from thermocouple and static-pressure measurements. The length of the light path through the box was 15.05 inches, and a density change of 0.5 percent of atmospheric density would cause a shift of approximately 1 fringe width. An observer would watch the screen and count the fringe shift as the pressure was slowly varied in the compartment.

Figure 12 shows the difference between the densities calculated from pressure and temperature measurements and those calculated from interferometer measurements for several compartment pressures. Each point represents an average of three visual readings taken for a particular fringe shift. The difference between all densities as determined by the two methods is less than approximately 0.5 percent. These data and the heated-plate data show that the diffraction-grating interferometer gives reliable and valid data and that the interferograms may be interpreted in the same manner as those obtained with a Mach-Zehnder interferometer.

Although the contrast of the fringes decreased as the fringe shift increased, the quality of the fringes was still usable at the greatest fringe shift. With available equipment, the pressure in the box could be increased or decreased sufficiently to produce over ±60 fringe shifts from undisturbed conditions. Thus, over 180 total interference fringes could be obtained with the grating interferometer by using the present light source. This number compares favorably with the maximum number of fringes that others have reported obtaining with a Mach-Zehnder interferometer. For example in reference 8, Ladenburg, Van Voorhis, and Winckler reported a maximum of 180 fringes with a magnesium spark in air. It was noted that, at the greatest fringe shift, fringes could still be observed over the complete view field when white light from the mercury lamp was used.

PRELIMINARY APPLICATION TO A SUPERSONIC CASCADE

An existing schlieren system which was used with a small supersonic cascade tunnel was converted to a grating interferometer. This preliminary application was made to determine the feasibility of using the instrument in practical experimental aerodynamics. In particular, it was desirable to determine the quality of the interferograms, the time involved for converting an existing schlieren system to an interferometer, and any difficulties which would occur in a practical application.

A schematic drawing of the test section showing the cascade blades and the position of the reference beam is shown in figure 13. The space below the side-wall plate is open to room conditions. The length L of the light rays through the test section is 2.25 inches. Figures 14 and 15 are typical interferograms taken with the interferometer. Figures 14(a) and 15(a) are interferograms taken before the tunnel was started. The curvature of the fringes in the undisturbed interferograms was caused by optical imperfections in the tunnel windows. The apparent semicircular bump on the convex surface of the bottom blade was caused by a chip in the glass. Part of the tubing between the static orifices on the blade and the manometer board can be seen connected to the convex

surface of the top blade. The dark straight line which partly covers the top blade is a shadow of the side-wall plate (see fig. 13). In the flow interferograms the area above this shadow has no particular meaning because the light in the reference beam has passed through an unknown density field. Figure 14(b) is an interferogram showing the flow through a passage formed by two cascade blades. The flow through this passage was slightly unstable especially downstream of the subsonic region following the shock which originated from the leading edge of the top blade. This instability was noted by watching the fringes shift on the view screen and by comparing several interferograms of the flow. Mercury manometer tubes which were connected to static orifices located on the concave surface of the upper blade did not record this instability. In order to obtain more steady flow, the bottom blade was removed. Figure 15(b) is an interferogram showing the flow around one blade. The flow is from left to right in all photographs. The stagnation pressure upstream of the shocks was approximately atmospheric. The nominal Mach number of the nozzle flow was 1.6. The photographic quality of the interferograms has proved to be satisfactory.

A comparison of the Mach number distribution along the concave surface of the top blade as calculated from the interferograms and as calculated from the pressure-orifice measurements on the blade is presented in figure 16. The Mach numbers from the interferograms were determined along an arbitrary line which was close to the blade surface but outside of the boundary layer. An approximation of the pressure loss through the various shocks was made by using existing shock equations. The reference point used in finding the fringe shift was taken under the first pressure tap from the leading edge of the top blade. The differences between the Mach numbers as determined by the two methods in figure 16(a) is probably explained by the lack of steady flow through the passage formed by the two blades. The Mach numbers as calculated from the interferograms are in good agreement with those calculated from static-pressure-orifice measurements when only one blade was located in the test section (fig. 16(b)).

The ability to measure conditions in unsteady or unstable flow is an advantage of the interference method. Other advantages of the interference method are that the flow is not disturbed by the measuring instrument and that the density distribution over a complete test area can be recorded instantaneously.

A relatively small amount of time was required to modify the existing equipment and to adjust the optical parts. For the information of the reader, the time involved from the beginning of the conversion until the first satisfactory interferogram was obtained was approximately 1 week. No particular difficulties were encountered in this practical application of the grating interferometer. The interferograms presented in this report were taken as soon as the tunnel was started because the air in

the reference beam near the test section was heated by prolonged running of the tunnel. In a refined apparatus, the reference beam could be passed through air insulated from the tunnel or, in some cases, the reference beam could be passed through a known constant-density field in front of the model. With the proper selection of mirrors and gratings, the view field could be made larger. Thus, the individual rays in the two beams which are recombined would be further separated at the test section.

CONCLUDING REMARKS

The investigation of a diffraction-grating interferometer has shown this apparatus to be a practical and very useful instrument for aerodynamic research. Features of this interferometer are low cost, easy adjustment, and large field of view.

Experimental data verified the ability of the instrument to provide valid and reliable measurements of air density. The interferograms obtained with a grating interferometer may be interpreted in the same manner as those obtained with a Mach-Zehnder interferometer. The grating interferometer was successfully applied to measurements within a small supersonic cascade tunnel. Interferograms taken of the flow within the tunnel yielded data which were in agreement with data obtained from pressure instruments.

Langley Aeronautical Laboratory,
National Advisory Committee for Aeronautics,
Langley Field, Va., September 19, 1952.

APPENDIX

FRINGE SPACING

The fringe spacing for a diffraction-grating interferometer can be determined analytically. A schematic drawing showing the two intersecting beams of parallel light that appear from the view screen to be existing in the vicinity of the disturbance area is presented in figure 17. Line a - a is an imaginary line which passes through the center of the lens unchanged in direction. The angles of deviation for all rays of any particular wavelength in any order are assumed to be equal. The first grating is assumed to be located at the focal point of the first lens. Consider the fringe spacing that would occur when the two beams of parallel light interfere. From the geometry of figure 2, it can be seen that, when two beams of parallel light interfere, the fringe spacing b as a first approximation is

$$b = \frac{\lambda}{\tan \alpha} \tag{A1}$$

since α is a small angle. From figure 17,

$$\tan \alpha = \frac{h}{f} \tag{A2}$$

and

$$h = x \tan \beta$$

or

$$h = x \frac{\sin \beta}{\sqrt{1 - \sin^2 \beta}} \tag{A3}$$

Angle β is equal to the diffraction angle θ for the ray perpendicular to the grating. Thus, equation (A3) can be written as

$$h = x \frac{\lambda/d}{\sqrt{1 - \frac{\lambda^2}{d^2}}} \tag{A4}$$

Combining equations (A1), (A2), and (A4) yields

$$b = \frac{fd}{x}\sqrt{1 - \frac{\lambda^2}{d^2}} \tag{A5}$$

The value of the radical is nearly equal to unity when d has values similar in magnitude to that used in this report. The fringe spacing for a diffraction-grating interferometer can thus usually be considered as independent of the wavelength of light.

This fact is also indicated by the equal fringe spacing of the interferograms presented in figure 18. These interferograms were taken with light of different wavelengths and, except for the wavelength adjustment of the monochromator, the adjustments of the interferometer remained constant. Variable-time exposures with a continuous light were used to obtain the desired film exposures.

REFERENCES

1. Kraushaar, R.: Diffraction Grating Interferometer. Jour. Optical Soc. Am. (Letters to the Editor), vol. 40, no. 7, July 1950, pp. 480-481.

2. Schardin, Hubert: Toepler's Schlieren Method. Basic Principles for Its Use and Quantitative Evaluation. Translation 156, The David W. Taylor Model Basin, U. S. Navy, July 1947.

3. Buchele, Donald R., and Day, Pierce B.: Interferometer With Large Working Field Utilizing Schlieren Optics. NACA RM E50I27, 1951.

4. Wood, Robert W.: Physical Optics. Third ed., The Macmillan Co., 1936, pp. 218-291.

5. Houstoun, R. A.: A Treatise of Light. Fourth ed., Longmans, Green and Co., 1925, pp. 154-185.

6. Schardin, H.: Theory and Applications of the Mach-Zehnder Interference-Refractometer. Univ. Texas, Defense Res. Lab., 1946.

7. Gooderum, Paul B., Wood, George P., and Brevoort, Maurice J.: Investigation With an Interferometer of the Turbulent Mixing of a Free Supersonic Jet. NACA Rep. 963, 1950. (Supersedes NACA TN 1857.)

8. Ladenburg, R., Van Voorhis, C. C., and Winckler, J.: Interferometric Study of Supersonic Phenomena. Part I: A Supersonic Air Jet at 60 LB/IN^2 Tank Pressure. NAVORD Rep. 69-46, Bur. Ordnance, Navy Dept., Apr. 17, 1946; Part II: The Gas Flow Around Various Objects in a Free Homogeneous Supersonic Air Stream. NAVORD Rep. 93-46, Sept. 2, 1946.

9. Ashkenas, Harry I., and Bryson, Arthur E.: Design and Performance of a Simple Interferometer for Wind-Tunnel Measurements. Jour. Aero. Sci., vol. 18, no. 2, Feb. 1951, pp. 82-90.

10. Edelman, Gilbert M.: The Design, Development, and Testing of Two-Dimensional Sharp-Cornered Supersonic Nozzles. Guided Missiles Program, M.I.T. Meteor Rep. No. 22, May 1, 1948.

11. Eckert, E. R. G., and Soehngen, E. E.: Studies on Heat Transfer in Laminar Free Convection With the Zehnder-Mach Interferometer. AF TR No. 5747, A.T.I. No. 44580, Air Materiel Command, U. S. Air Force, Dec. 27, 1948.

12. Howes, Walton L., and Buchele, Donald R.: A Theory and Method for Applying Interferometry to the Measurement of Certain Two-Dimensional Gaseous Density Fields. NACA TN 2693, 1952.

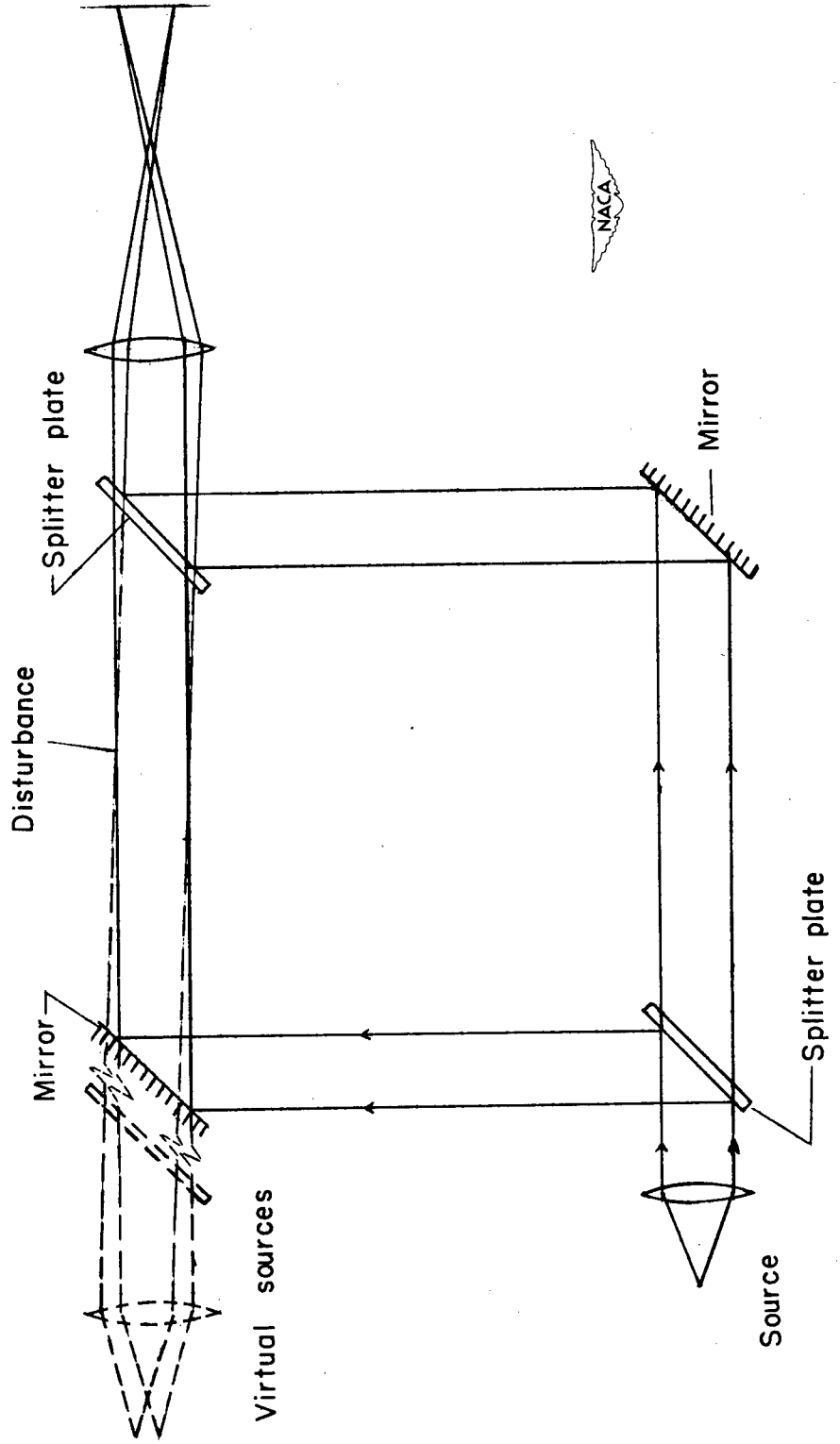

Figure 1.- A Mach-Zehnder interferometer.

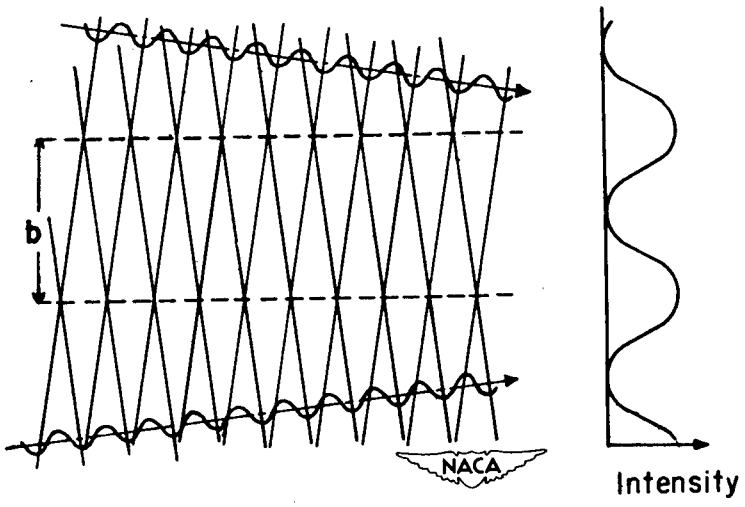

Figure 2.- Formation of fringes.

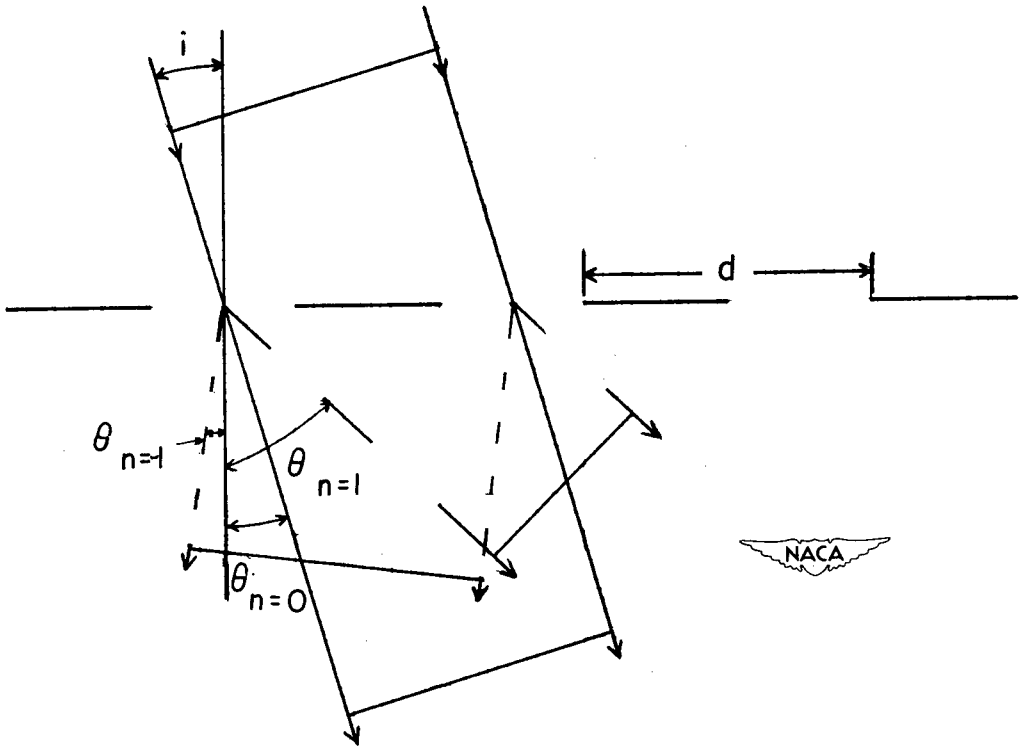

Figure 3.- A parallel light beam passing through a diffraction grating.

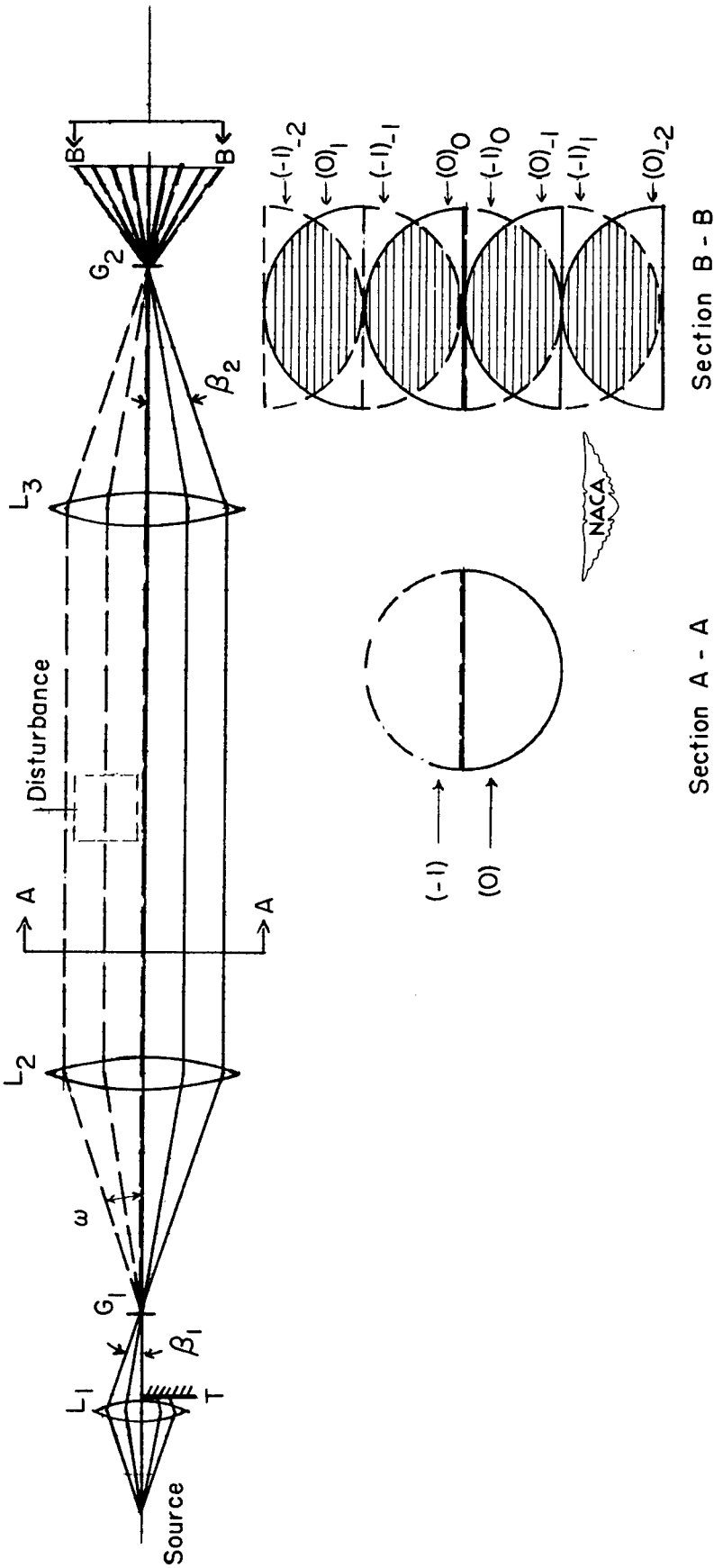

Figure 4.- Diffraction-grating interferometer.

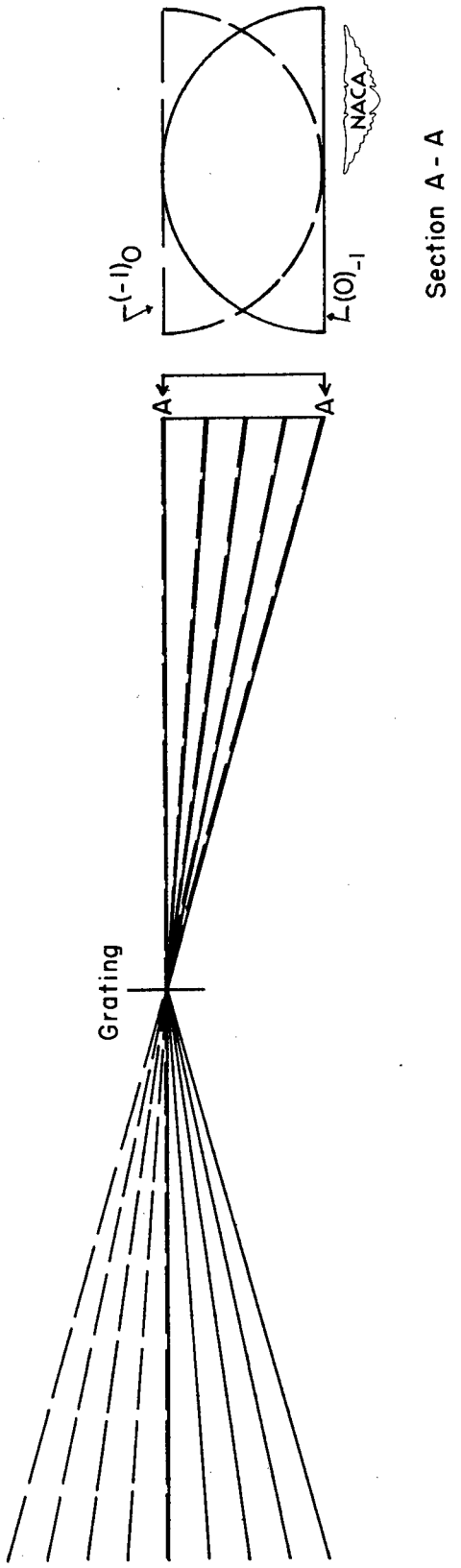

(a) The infinite fringe.

Figure 5.- Light rays near second grating. (First grating at image of light source.)

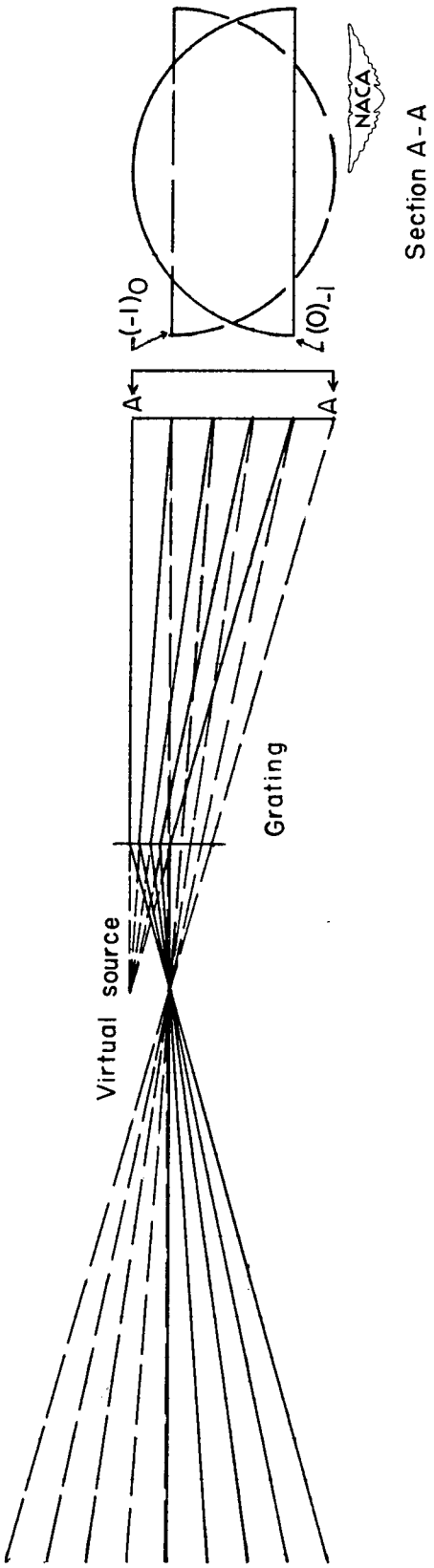

(b) Finite fringes.

Figure 5.- Concluded.

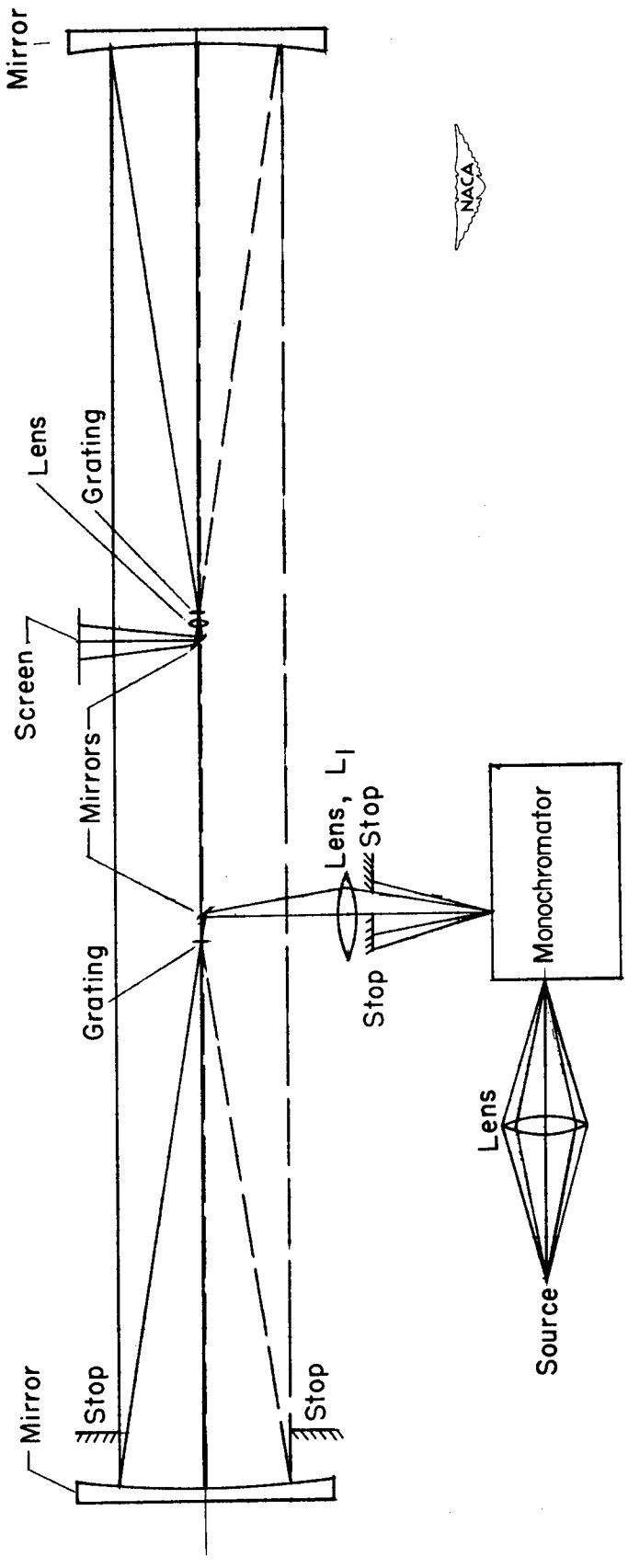

Figure 6.- Schematic drawing of interferometer actually used.

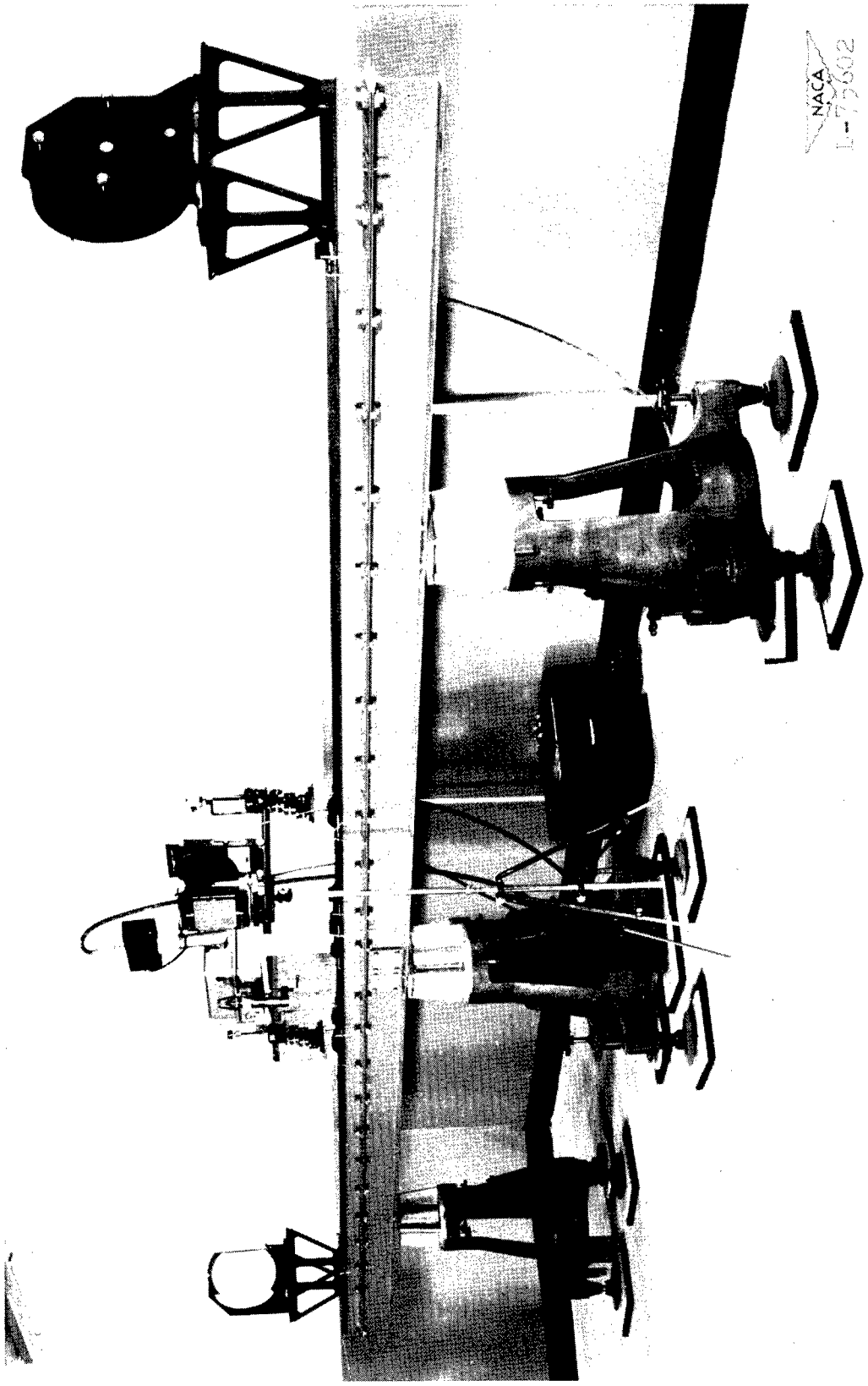

Figure 7.- Photograph of diffraction-grating interferometer.

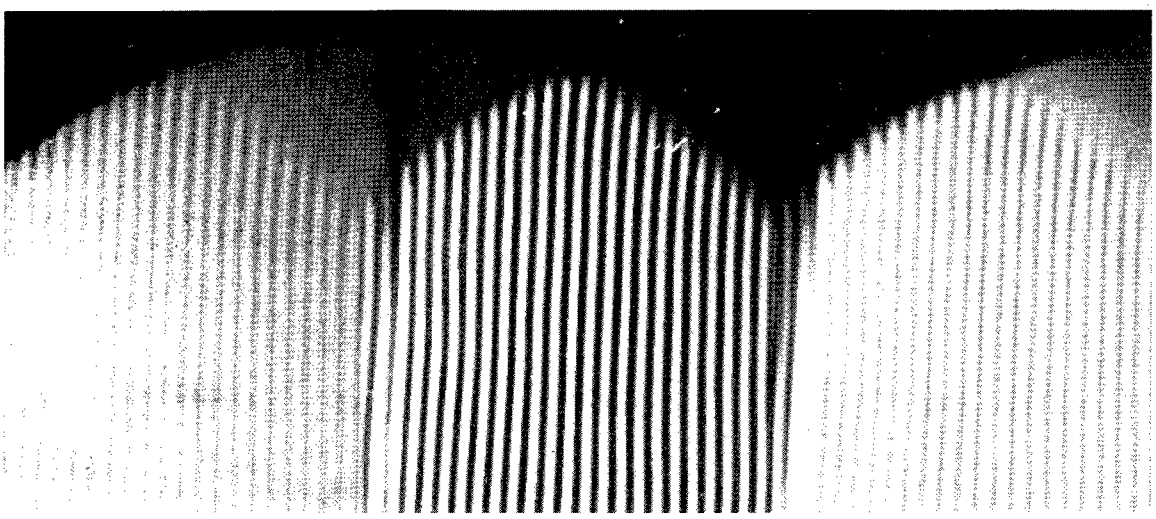

Figure 8.- Three of the images occurring at the film plate.

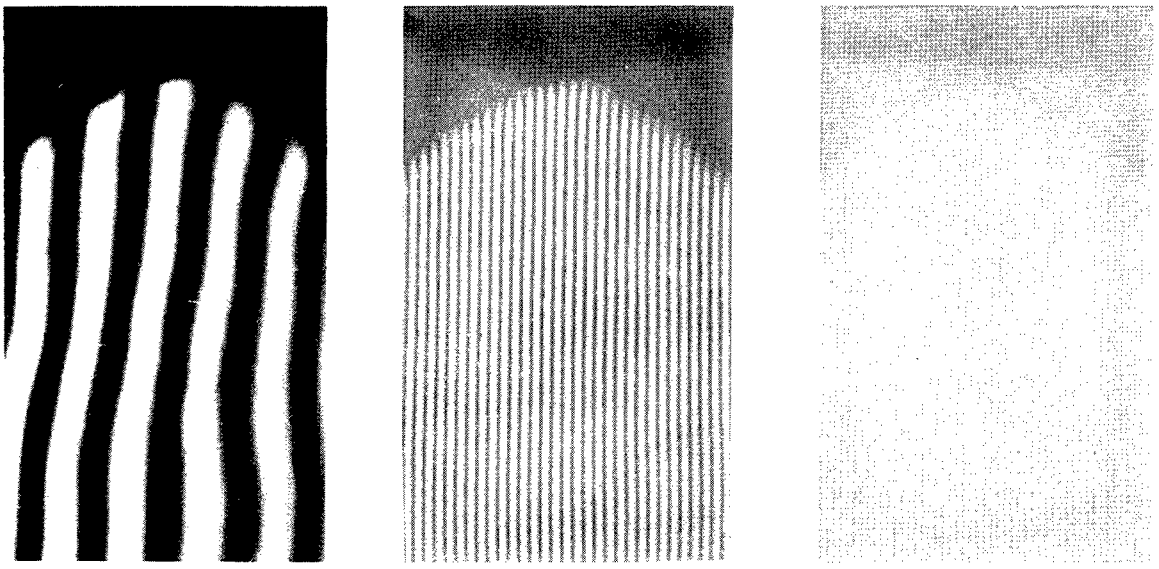

a) 1.5 fringes per inch. (b) 8 fringes per inch. (c) 13 fringes per inch.

Figure 9.- Examples of different fringe spacings. L-76968

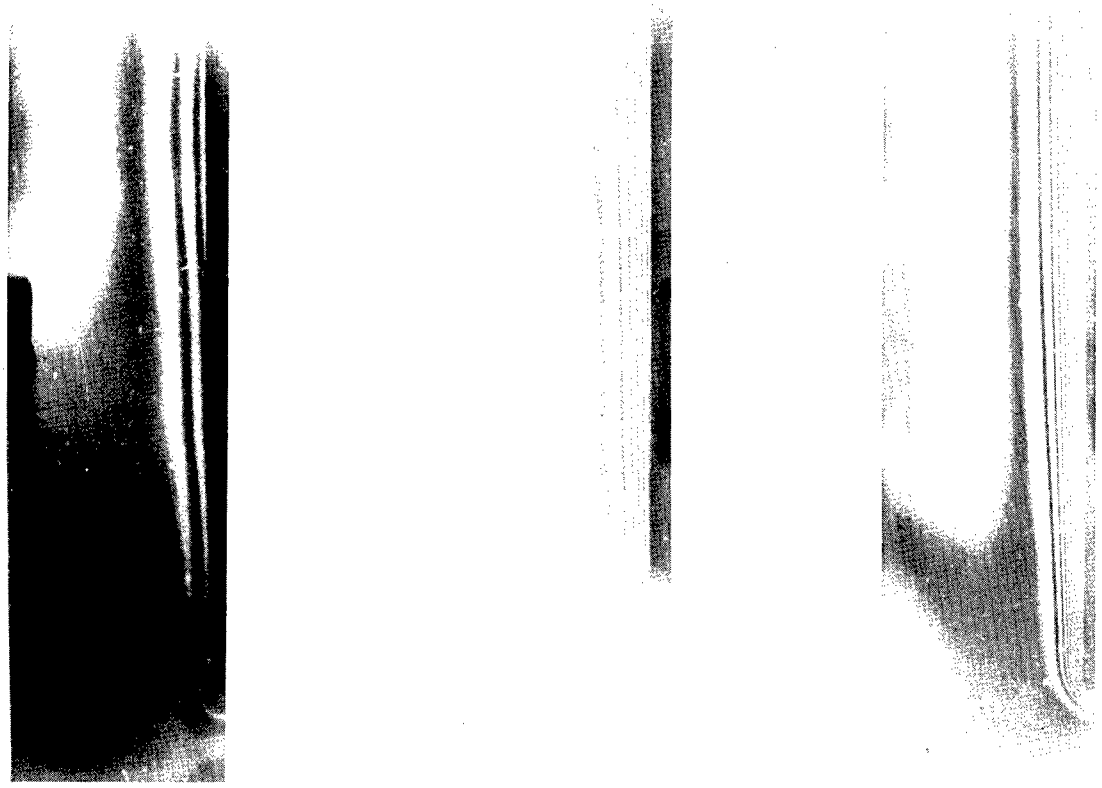

NACA
L-76969

(a) $T' - T = 6^{\circ}$ F. (b) $T' - T = 21^{\circ}$ F. (c) $T' - T = 46^{\circ}$ F.

Figure 10.- Interferograms of a heated plate at several temperatures.

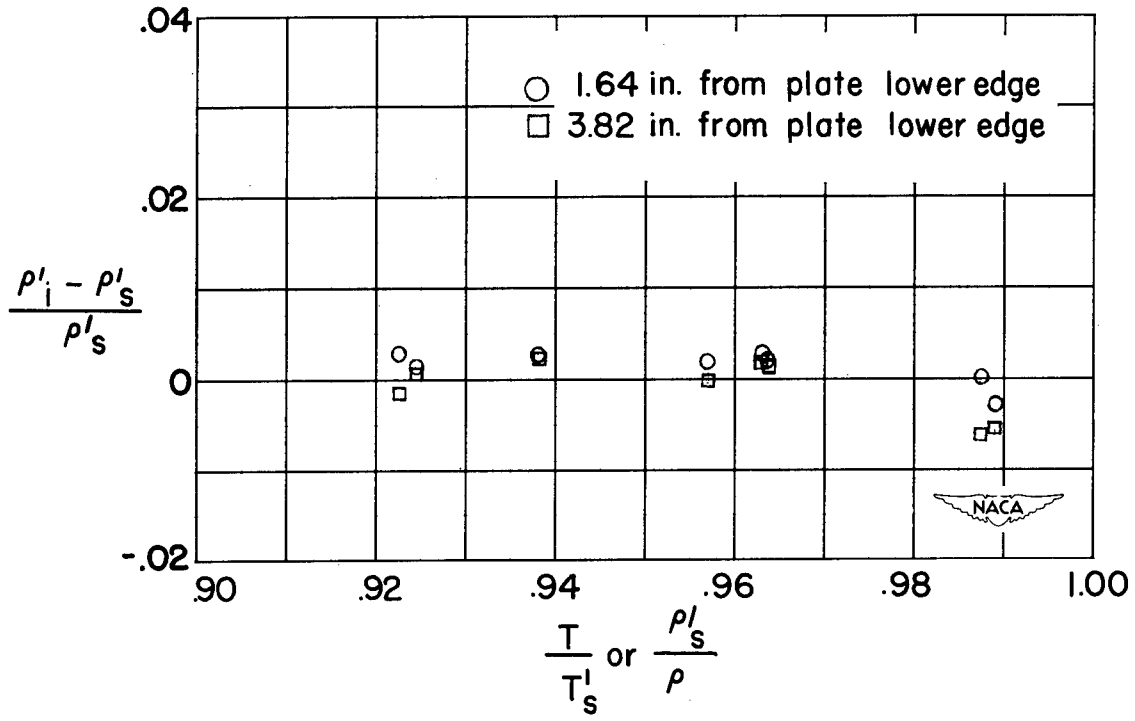

Figure 11.- Differences between measured densities at a heated plate.

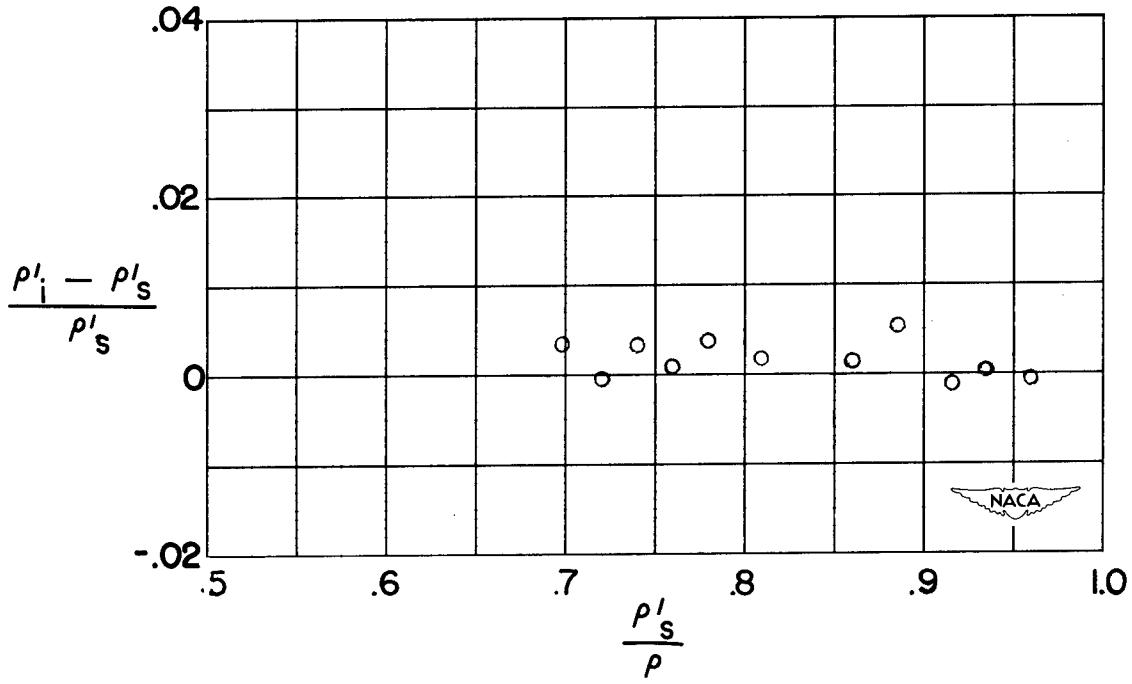

Figure 12.- Differences between measured densities in a box.

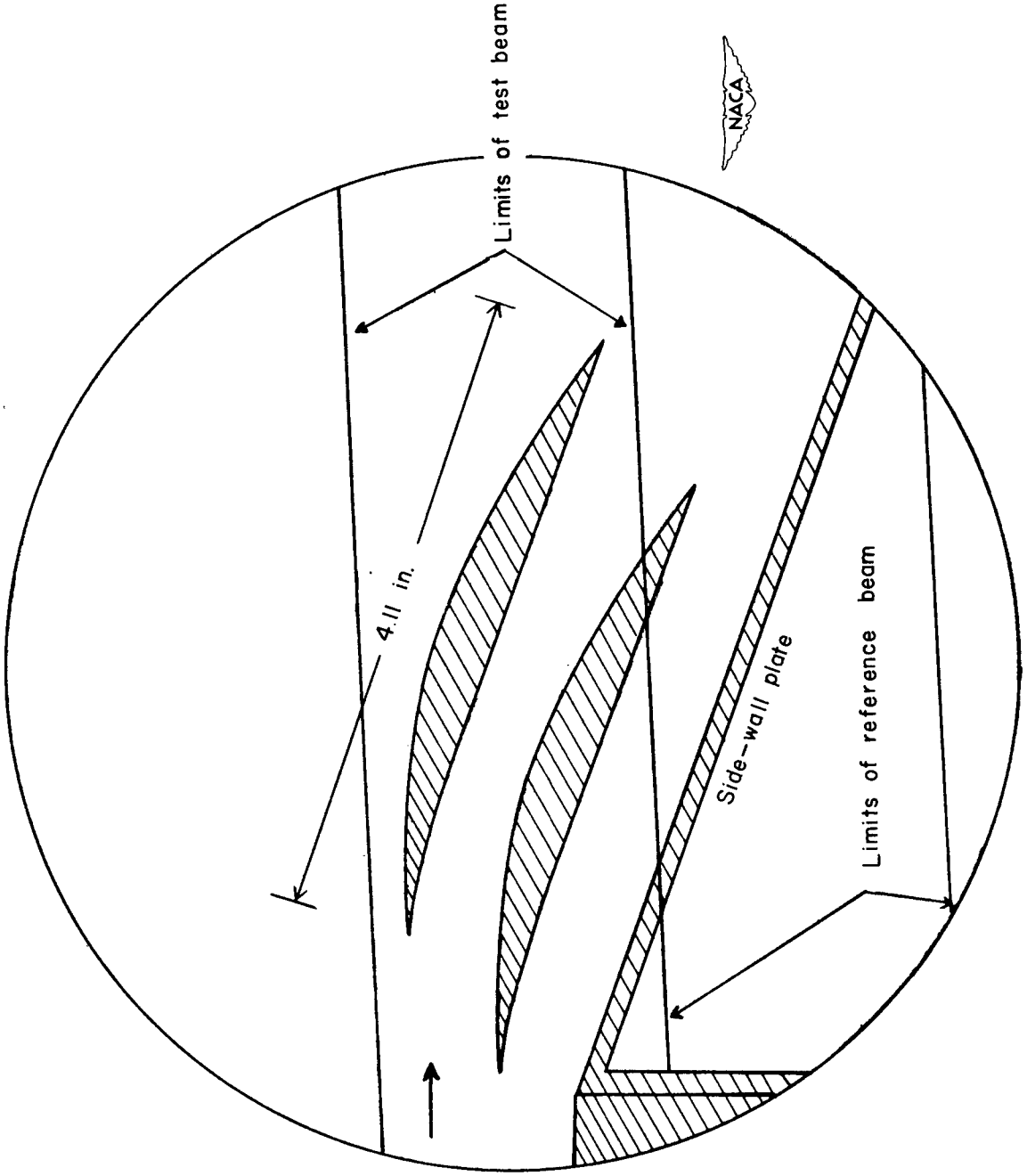

Figure 13.- Sketch of test section of supersonic cascade tunnel.

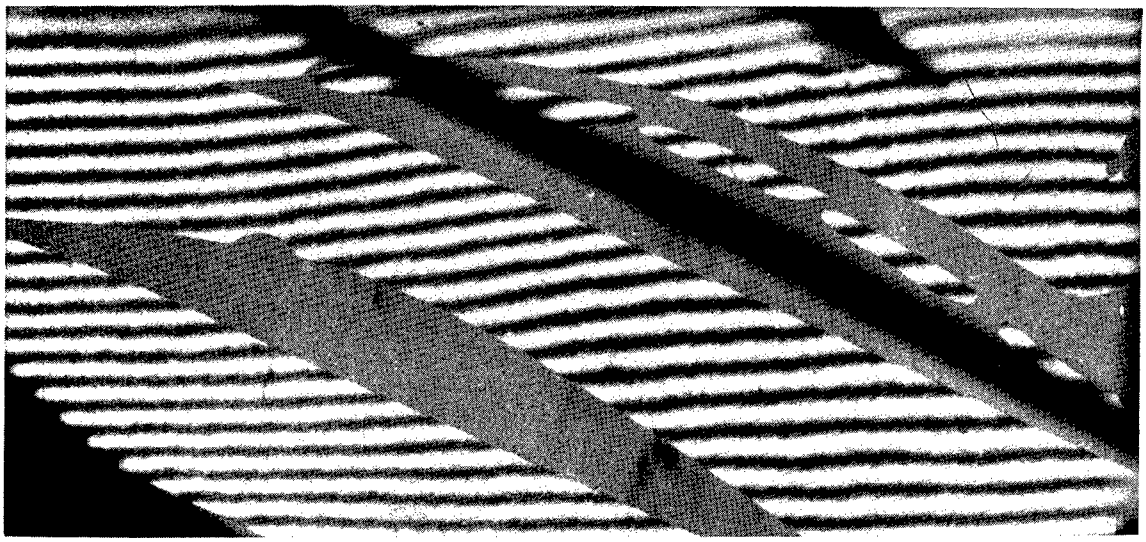

(a) Undisturbed fringes.

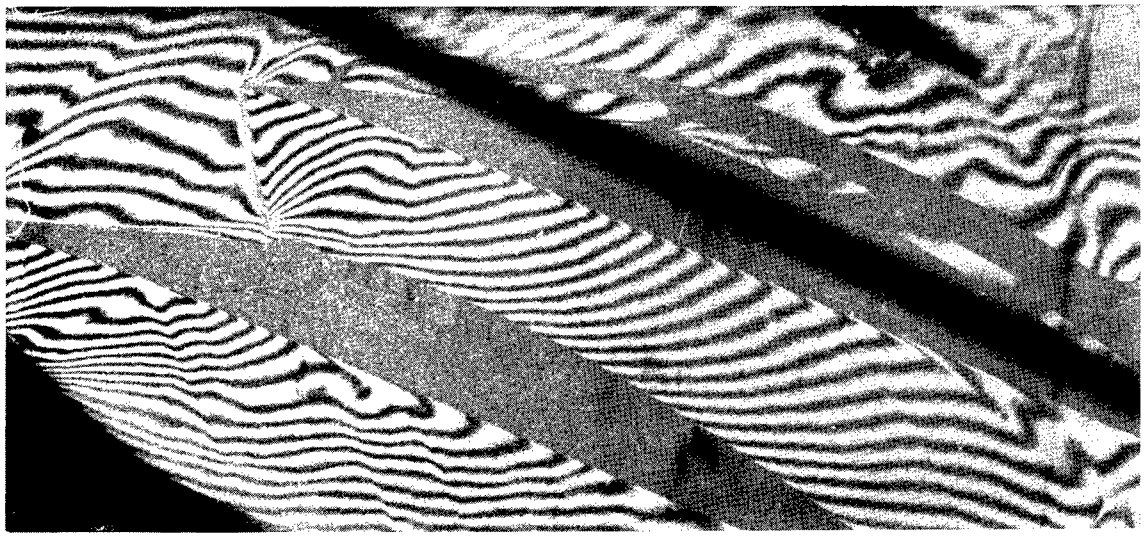

(b) Fringes with flow.

NACA L-76970

Figure 14.- Interferograms taken with two blades in passage.

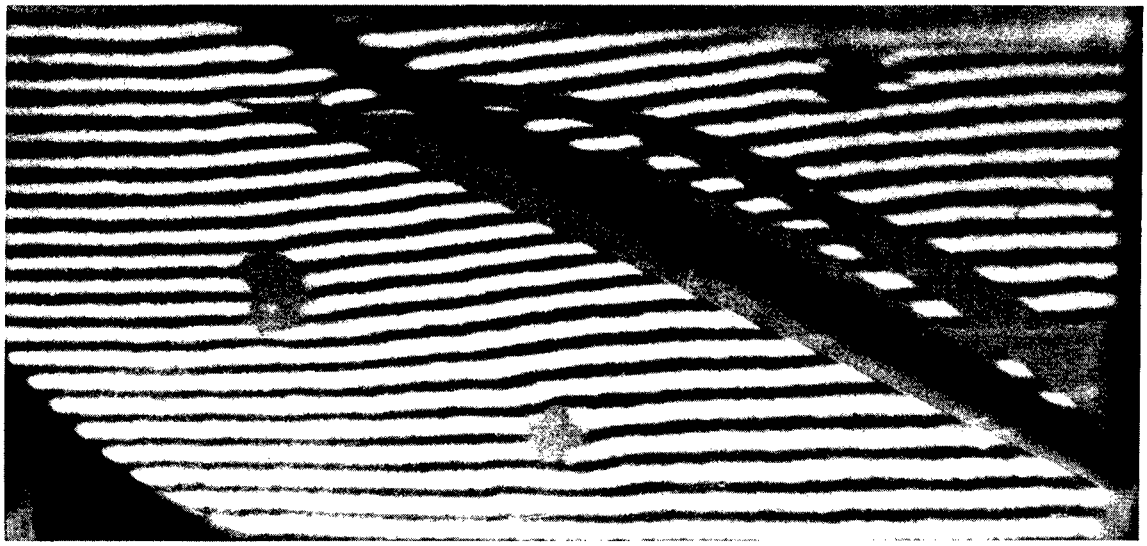

(a) Undisturbed fringes.

(b) Fringes with flow.

NACA
L-76971

Figure 15.- Interferograms taken with one blade in passage.

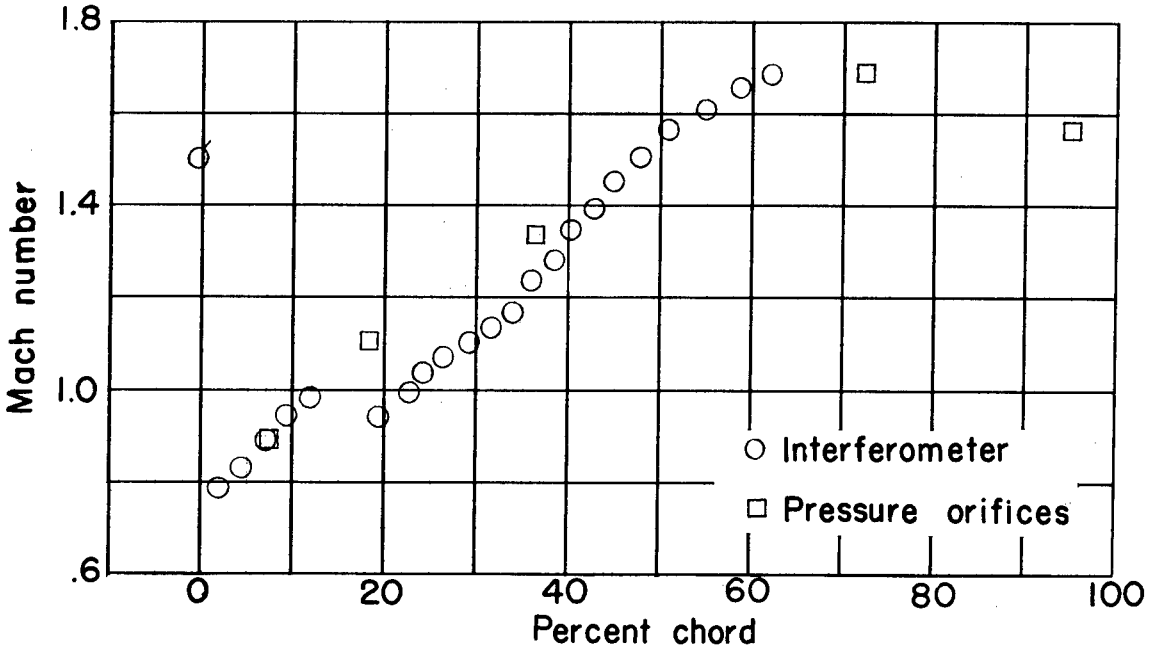

(a) Two blades in passage (see fig. 14).

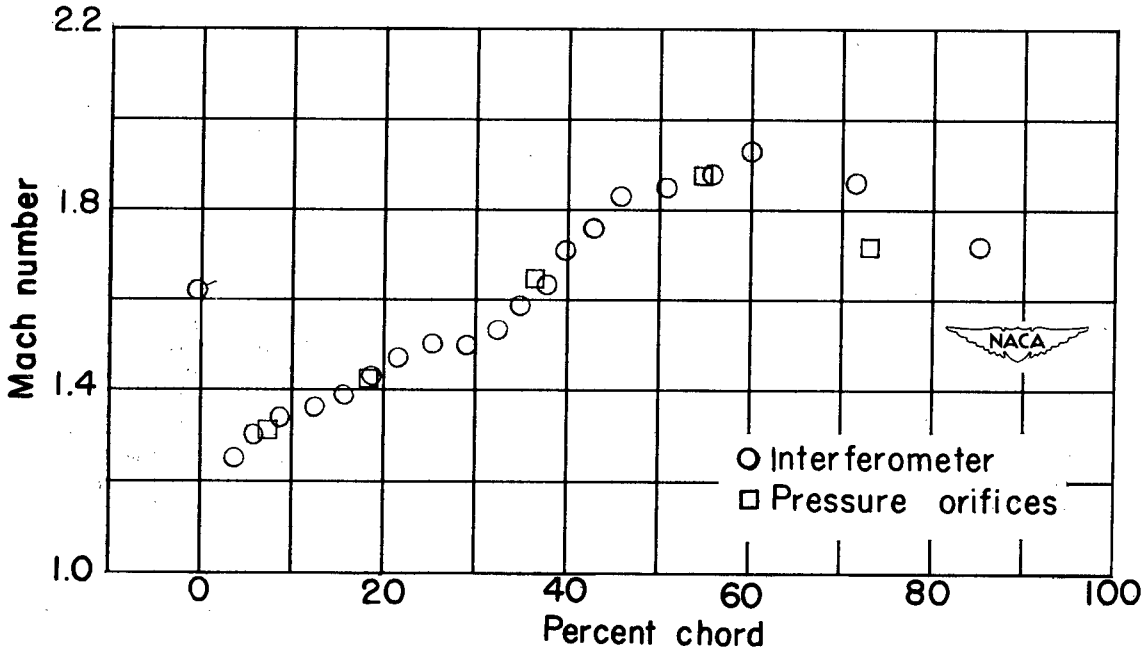

(b) One blade in passage (see fig. 15).

Figure 16.- Mach number distribution along concave surface of top blade. (Flagged test points slightly ahead of blade.)

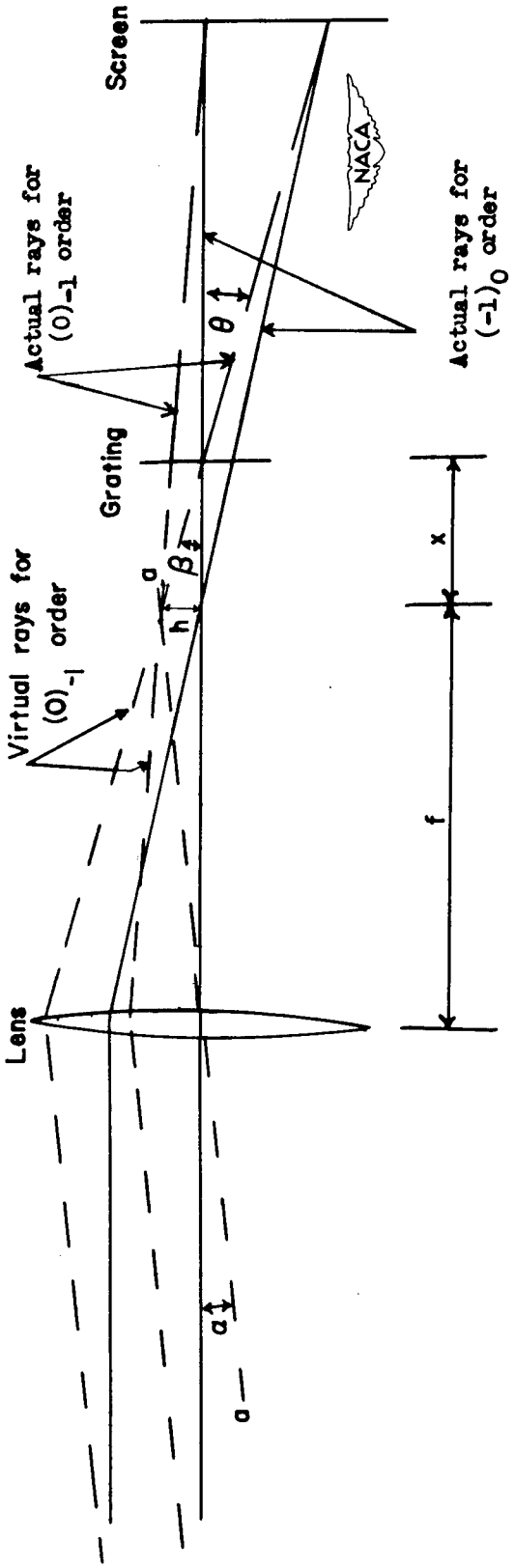

Figure 17.- Apparent intersection of parallel rays for a grating interferometer.

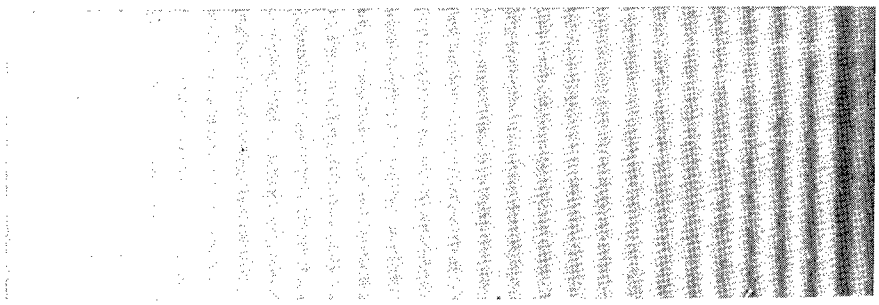

(a) Red light.

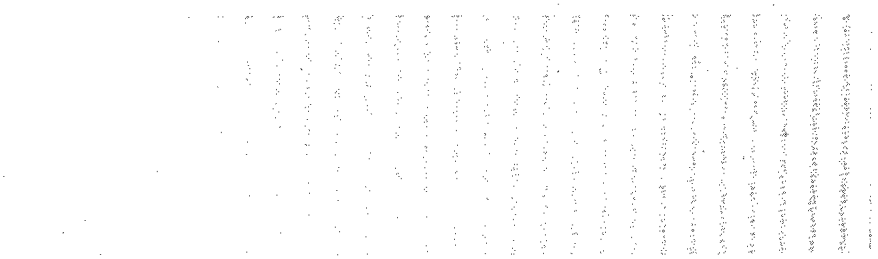

(b) Green light.

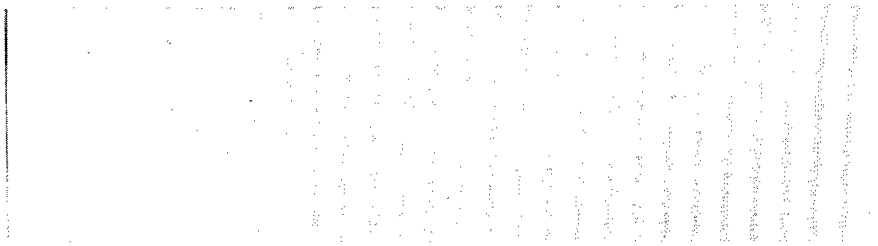

(c) Blue light.

L-76972

Figure 18.- Interferograms taken with light of different wavelengths.

NACA-Langley - 11-3-52 - 1000

NACA TN 2827
National Advisory Committee for Aeronautics.
INVESTIGATION OF A DIFFRACTION-GRATING INTERFEROMETER FOR USE IN AERODYNAMIC RESEARCH. James R. Sterrett and John R. Erwin. November 1952. 36p. photos., diagrs. (NACA TN 2827)

A low-cost interferometer that is easy to adjust and has a large field of view is described. This instrument, which is based on a principle discovered by Kraushaar, uses small diffraction gratings to produce and recombine separate beams of light. The usual two-parabolic-mirror schlieren system can be converted inexpensively into a diffraction-grating interferometer. Experimental data are presented to verify the ability of the instrument to provide valid and reliable measurements of air density. Photographs of the flow in a supersonic cascade tun-

Copies obtainable from NACA, Washington (over)

1. Instruments, Laboratory (8.2)
2. Research Equipment (9.1)

I. Sterrett, James R.
II. Erwin, John R.
III. NACA TN 2827

NACA TN 2827
National Advisory Committee for Aeronautics.
INVESTIGATION OF A DIFFRACTION-GRATING INTERFEROMETER FOR USE IN AERODYNAMIC RESEARCH. James R. Sterrett and John R. Erwin. November 1952. 36p. photos., diagrs. (NACA TN 2827)

A low-cost interferometer that is easy to adjust and has a large field of view is described. This instrument, which is based on a principle discovered by Kraushaar, uses small diffraction gratings to produce and recombine separate beams of light. The usual two-parabolic-mirror schlieren system can be converted inexpensively into a diffraction-grating interferometer. Experimental data are presented to verify the ability of the instrument to provide valid and reliable measurements of air density. Photographs of the flow in a supersonic cascade tun-

Copies obtainable from NACA, Washington (over)

1. Instruments, Laboratory (8.2)
2. Research Equipment (9.1)

I. Sterrett, James R.
II. Erwin, John R.
III. NACA TN 2827

NACA TN 2827
National Advisory Committee for Aeronautics.
INVESTIGATION OF A DIFFRACTION-GRATING INTERFEROMETER FOR USE IN AERODYNAMIC RESEARCH. James R. Sterrett and John R. Erwin. November 1952. 36p. photos., diagrs. (NACA TN 2827)

A low-cost interferometer that is easy to adjust and has a large field of view is described. This instrument, which is based on a principle discovered by Kraushaar, uses small diffraction gratings to produce and recombine separate beams of light. The usual two-parabolic-mirror schlieren system can be converted inexpensively into a diffraction-grating interferometer. Experimental data are presented to verify the ability of the instrument to provide valid and reliable measurements of air density. Photographs of the flow in a supersonic cascade tun-

Copies obtainable from NACA, Washington (over)

1. Instruments, Laboratory (8.2)
2. Research Equipment (9.1)

I. Sterrett, James R.
II. Erwin, John R.
III. NACA TN 2827

NACA TN 2827
National Advisory Committee for Aeronautics.
INVESTIGATION OF A DIFFRACTION-GRATING INTERFEROMETER FOR USE IN AERODYNAMIC RESEARCH. James R. Sterrett and John R. Erwin. November 1952. 36p. photos., diagrs. (NACA TN 2827)

A low-cost interferometer that is easy to adjust and has a large field of view is described. This instrument, which is based on a principle discovered by Kraushaar, uses small diffraction gratings to produce and recombine separate beams of light. The usual two-parabolic-mirror schlieren system can be converted inexpensively into a diffraction-grating interferometer. Experimental data are presented to verify the ability of the instrument to provide valid and reliable measurements of air density. Photographs of the flow in a supersonic cascade tun-

Copies obtainable from NACA, Washington (over)

1. Instruments, Laboratory (8.2)
2. Research Equipment (9.1)

I. Sterrett, James R.
II. Erwin, John R.
III. NACA TN 2827

NACA TN 2827

nel are included to indicate the quality of the interferograms obtained.

NACA TN 2827

nel are included to indicate the quality of the interferograms obtained.

Copies obtainable from NACA, Washington

NACA TN 2827

nel are included to indicate the quality of the interferograms obtained.

Copies obtainable from NACA, Washington

NACA TN 2827

nel are included to indicate the quality of the interferograms obtained.

Copies obtainable from NACA, Washington